

Supplemental online content for:

Exceptional Response to Temsirolimus in a Metastatic Clear Cell Renal Cell Carcinoma With an Early Novel *MTOR*-Activating Mutation

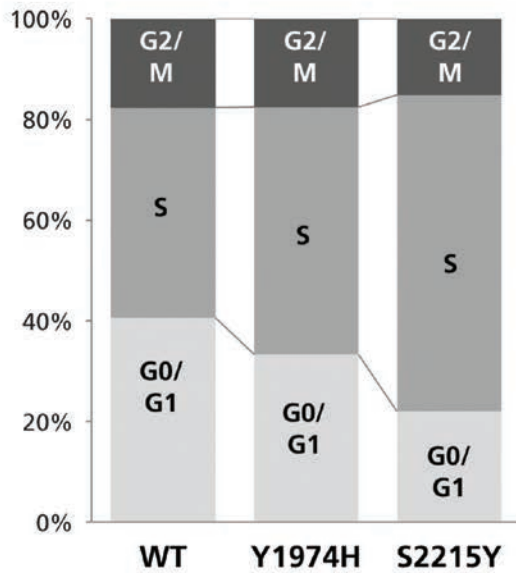
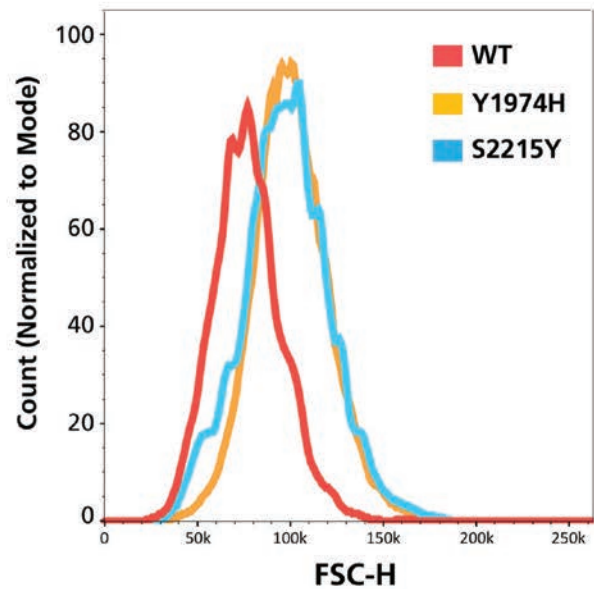
*Juan Francisco Rodríguez-Moreno, MD; María Apellaniz-Ruiz, PhD;
Juan María Roldan-Romero, MS; Ignacio Durán, MD; Luis Beltrán, MD;
Cristina Montero-Conde, PhD; Alberto Cascón, PhD; Mercedes Robledo, PhD;
Jesus García-Donas, MD, PhD; and Cristina Rodríguez-Antona, PhD*

J Natl Compr Canc Netw 2017;15(11):1310–1315

eFigure 1: *MTOR* Mutation Effects on Cell Cycle and Forward Scatter

eTable 1: Nonsynonymous Coding and LOF Variants Detected in the Tumors of the Patient (Primary Tumor and Metastasis) and Absent in the Blood

eAppendix 1: Supplementary Materials

A**B**

eFigure 1. *MTOR* mutation effects on cell cycle and forward scatter. HEK293 cells transfected with pCDNA3-FLAG-mTOR (wild-type, Y1974H or S2215Y) were subjected to serum starvation. After trypsinization, the cells were fixed and cellular DNA stained with propidium iodide. The transfected cells, which were found to be FLAG-positive, were analyzed on a FACS CANTO II for (A) DNA content using propidium iodide and (B) forward scatter pattern.

eTable 1. Nonsynonymous Coding and LOF Variants Detected in the Tumors of the Patient (Primary Tumor and Metastasis) and Absent in the Blood

Gene	Variant	Ref. Allele	Alt. Allele	Primary T1_AF	Primary T2_AF	Primary T3_AF	Metastasis_AF	Effect	Amino_Acid_Change
ACACB	12:109670522	C	A	0.31	0.20	0.22	0.33	MISSENSE	S1280R;S13350R;S13350R
ADAL	15:43643188	C	A	0.36	0.18	0.32	0.31	MISSENSE	D274E;D274E
ADAM28	8:24181384	G	A	0.17				MISSENSE	G253D
ADAMTSL4	1:150526429	G	A	0.20				MISSENSE	G321E;G321E;G321E
AJAP1	1:4772367	C	T		0.17			MISSENSE	P146L;P146L
AK2	1:33487194	C	T	0.17				MISSENSE	M110I;M110I;M110I
ALS2CR11	2:202358161	C	T	0.20				MISSENSE	G968E
ANKRD18B	9:33541216	G	C	0.33	0.23	0.24		MISSENSE	G294R
APO01468.1	21:47613570	T	C	0.45	0.31			MISSENSE	H35R
APOBEC3C	22:39411749	G	A		0.22			MISSENSE	R56Q
ARHGAP22	10:49658586	C	A		0.27			MISSENSE	C529F;C535F;C545F
ARID2	12:46245092	G	T	0.36	0.28	0.41	0.28	MISSENSE	Q1062H
ARL14EP	11:30352649	G	A	0.23				MISSENSE	G52R
ARMC4	10:28250610	C	A		0.29	0.24	0.14	MISSENSE	D425Y
ARX	X:25025243	C	G	0.64	0.48	0.42	0.57	MISSENSE	S478T
ATHL1	11:289880	C	G	0.44	0.33	0.51	0.38	MISSENSE	L22V;L22V
ATP9B	18:76886357	AG	A	0.26		0.21	0.21	FRAME_SHIFT	
BAP1	3:52437801	CTTT	CTTTT	0.34	0.16	0.28	0.26	FRAME_SHIFT	
BCL11B	14:99641956	G	A	0.27				MISSENSE	T212M;T335M;T406M
BSCL2	11:62472862	C	A	0.39	0.18	0.19	0.40	MISSENSE	L105F;L105F;L105F;L41F;L41F;L41F;L41F
C4orf21	4:113539720	G	A	0.18				MISSENSE	S493F
C7orf55-LUC7L	7:139092020	G	T	0.26	0.16	0.25	0.30	MISSENSE	R204I;R270I
CARD16	11:104915222	C	A		0.18			MISSENSE	L57F;L57F;L57F
CCNG1	5:162868187	G	A	0.13				MISSENSE	R123Q;R123Q
CDC14B	9:99296337	A	T	0.38	0.22	0.24	0.51	MISSENSE	F273Y;F273Y;F273Y
CELF2	10:11259399	G	A		0.22			MISSENSE	V64I;V64I;V64I;V64I;V64I;V64I
CFH	1:196715027	G	A	0.20				MISSENSE	A1131T
CHUK	10:101950628	T	A	0.42	0.29	0.34	0.34	MISSENSE	M736L
CIC	19:42795216	G	T	0.15				MISSENSE	G1675C;G766C;G766C
CILP2	19:19656719	C	T			0.16		MISSENSE	P1122L;P1128L
CKAP5	11:46786695	C	A	0.20				NONSENSE	E1175*
CLSPN	1:36219445	T	G	0.39	0.24	0.30	0.20	MISSENSE	K558Q;K558Q;K558Q
CNKSR1	1:26511636	G	A		0.15			MISSENSE	V423M;V430M
CPNE2	16:57144689	C	T	0.57	0.32	0.29	0.19	MISSENSE	A12V;A12V;A12V
CTR9	11:10781764	A	G	0.37	0.20	0.18	0.24	MISSENSE	K213E
CTSH	15:79224788	T	G			0.14		MISSENSE	S140R
CXorf23	X:19971111	C	T	0.20				MISSENSE	E542K;E542K;E542K
CYP2A6	19:41355828	C	T	0.12				MISSENSE	V80M
DDX46	5:134131842	T	A	0.17				SPLICE_SITE_DONOR	
DEF6	6:35286030	C	T		0.21			MISSENSE	R333W
DENND3	8:142185453	G	T	0.42	0.22	0.22	0.37	MISSENSE	K730N;K810N
DHRS4	14:24424266	C	T	0.25				MISSENSE	R51C
DHX30	3:47891435	T	A	0.46	0.33	0.42	0.56	MISSENSE	L1098Q;L1137Q
DHX40	17:57679913	G	T	0.18				MISSENSE	G613C
DIDO1	20:61512104	G	A	0.20				MISSENSE	P1735L;P1735L
DNAH6	2:85011924	A	T	0.43	0.24	0.34	0.32	MISSENSE	N3648I;N3648I
DOCK11	X:117676803	C	T	0.17				MISSENSE	S73F;S73F
EEA1	12:93226564	A	T	0.18				MISSENSE	N326K
EIF4G3	1:21268389	C	T	0.18				MISSENSE	E364K;E364K;E370K;E370K
EML4	2:42510010	C	T	0.19				MISSENSE	P222L;P280L;P291L
FCGBP	19:40424297	A	T	0.36	0.20	0.30	0.34	MISSENSE	F636I
FER1L6	8:124975587	T	C	0.29	0.25	0.34	0.23	MISSENSE	V49A;V49A
GAK	4:861013	G	A	0.20				MISSENSE	P868L
GLT6D1	9:138516493	G	A	0.23	0.24	0.32		MISSENSE	P94L
GOLPH3L	1:150620846	C	G	0.61	0.27	0.37	0.47	MISSENSE	S270T
HAS1	19:52216790	C	T	0.19				MISSENSE	A542T;A543T;A550T
HCAR3	12:123200354	G	A		0.69		0.38	MISSENSE	R311C
HLA-DOA	6:32975808	G	A	0.25	0.36	0.33	0.39	MISSENSE	R105C
HLA-DRB1	6:32549540	C	T	0.20	0.21	0.15		MISSENSE	S149N
HLA-DRB1	6:32549531	T	C			0.15		MISSENSE	Y152C
HLA-DRB1	6:32549525	C	G			0.15		MISSENSE	G154A
HNRNPLL	2:38812862	C	T	0.35		0.32	0.37	MISSENSE	G157E;G157E
HS6ST2	X:131842613	A	G			0.14		MISSENSE	M1T
HSD17B14	19:49316771	T	C	0.33	0.19	0.27	0.38	MISSENSE	E194G
IGHMBP2	11:68676003	G	T		0.15			MISSENSE	A151S
IGHV3-35	14:106845586	A	C	0.43	0.14			MISSENSE	L30V
IGHV3-35	14:106845579	T	C	0.30				MISSENSE	Q32R
INPP4B	4:143235912	G	A	0.19				NONSENSE	R126*;R126*;R126*;R126*
IRAK1	X:153284141	G	A	0.14				MISSENSE	S213L;S213L
KLHL20	1:173744950	C	T	0.21	0.21	0.14	0.27	MISSENSE	P536L
KLHL28	14:45414636	C	T	0.28	0.19	0.25	0.28	MISSENSE	A166T

(continued)

eTable 1. Nonsynonymous Coding and LOF Variants Detected in the Tumors of the Patient (Primary Tumor and Metastasis) and Absent in the Blood (cont.)

Transcript_ID
ENST00000377854;ENST00000338432;ENST00000377848
ENST00000422466;ENST00000562188
ENST00000265769
ENST00000271643;ENST00000369038;ENST00000369039
ENST00000378190;ENST00000378191
ENST00000373449;ENST00000467905;ENST00000354858
ENST00000439140
ENST00000290943
ENST00000594486
ENST00000361441
ENST00000249601;ENST00000435790;ENST00000417912
ENST00000334344
ENST00000282032
ENST00000305242
ENST00000379044
ENST00000409548;ENST00000409479
ENST00000307671
ENST00000460680
ENST00000443726;ENST00000345514;ENST00000357195
ENST00000360796;ENST00000433053;ENST00000405837;ENST00000278893;ENST00000403550;ENST00000407022;ENST00000421906
ENST00000505019
ENST00000354926;ENST00000541515
ENST00000375706;ENST00000375704;ENST00000525374
ENST00000340828;ENST00000393929
ENST00000375236;ENST00000463569;ENST00000375241
ENST00000417956;ENST00000608830;ENST00000315874;ENST00000354440;ENST00000399850;ENST00000427450
ENST00000367429
ENST00000370397
ENST00000572681;ENST00000160740;ENST00000575354
ENST00000291495;ENST00000586018
ENST00000529230
ENST00000520551;ENST00000251195;ENST00000318121
ENST00000361530;ENST00000374253
ENST00000290776;ENST00000535318;ENST00000565874
ENST00000361367
ENST00000220166
ENST00000356980;ENST00000379687;ENST00000379682
ENST00000301141
ENST00000354283;ENST00000452510
ENST00000316637
ENST00000262585;ENST00000519811
ENST00000313250
ENST00000446256;ENST00000445061
ENST00000251241
ENST00000266070;ENST00000395343
ENST00000237449;ENST00000389394
ENST00000276202;ENST00000276204
ENST00000322349
ENST00000264211;ENST00000400422;ENST00000374937;ENST00000602326
ENST00000402711;ENST00000318522;ENST00000401738
ENST00000221347
ENST00000399018;ENST00000522917
ENST00000314167
ENST00000371763
ENST00000271732
ENST00000540069;ENST00000222115;ENST00000601714
ENST00000528880
ENST00000229829
ENST00000360004
ENST00000360004
ENST00000360004
ENST00000449105;ENST00000608859
ENST00000406696
ENST00000263278
ENST00000255078
ENST00000390617
ENST00000390617
ENST00000262992;ENST00000308502;ENST00000508116;ENST00000513000
ENST00000393687;ENST00000369980
ENST00000209884
ENST00000396128

eAppendix 1. Supplementary Material

Material and DNA Extraction

Samples available for the study included 3 different regions of the primary tumor obtained from the nephrectomy before temsirolimus treatment; tissue from a single bone metastasis that appeared 7 years after temsirolimus treatment initiation and that was surgically removed; and from the peripheral blood from the patient. DNA was isolated from the formalin-fixed paraffin-embedded (FFPE) tumor tissues using DNeasy Blood & Tissue Kit (QIAGEN) and from the peripheral blood using the FlexiGene DNA Kit (QIAGEN).

The project was approved by the Instituto de Salud Carlos III Review Board, and the patient provided written informed consent to participate in the study.

Whole-Exome Sequencing

Whole-exome sequencing (WES) was performed on the 3 regions of the primary tumor and on the metastasis and blood of the patient at the National Centre for Genomic Analysis, as described previously.¹ Briefly, the Covaris S2 System (Covaris, Woburn, MA) was applied for DNA fragmentation, and exome capture was performed using the SureSelect XT HumanAllExon V5 kit (Agilent Technologies, Santa Clara, CA). Exome sequencing was performed using 100-base paired-end technology in a HiSeq2000 (Illumina, San Diego, CA). The mean depth of coverage was >80x in all samples. Tumor variants were defined as those detected in the tumor DNA but not in the blood DNA. Metastatic-specific tumor mutations were those detected in the metastasis DNA but not in the primary tumor. An allele frequency threshold of 0.10 was applied. Variants were manually curated and relevant mutations were confirmed by Sanger sequencing with an ABI PRISM 3700 DNA Analyzer capillary sequencer (Applied Biosystems, Foster City, CA). In addition, *MTOR* introns 41–46 were sequenced by Sanger in the primary tumor and metastatic sample. Primers are available on request.

Experimental Analysis

A wild-type human *MTOR* expression construct (pCDNA3-Flag-mTOR) was acquired from Addgene (Cambridge MA; plasmid #26603). Site-directed mu-

tagenesis was performed in pCDNA3-Flag-mTOR to generate Y1974H and S2215Y point mutations (DNA Express Inc, Montreal, Quebec, Canada).

Functional assessment of mTOR pY1974H variant was performed in HEK293 cells. Cells were transfected with pCDNA3-Flag-mTOR, pCDNA3-Flag-mTOR-Y1974H, or pCDNA3-Flag-mTOR-S2215Y using Lipofectamine 2000 (Life Technologies, Carlsbad, CA) according to the manufacturer's instructions, and 24 hours after transfection cells were serum-starved for 24 hours, and then stimulated with 1% or 10% fetal bovine serum for 2 hours. To block the mTOR pathway, cells were treated with 2.5, 12.5, and 100 nM of rapamycin (Apollo Scientific, Bredbury, Stockport, UK) for 6 hours. Cells were lysed in RIPA buffer (Sigma-Aldrich, St. Louis, MO) with Phosphatase Inhibitor Cocktail 2 and 3 (Sigma-Aldrich, P5726 and P0044) and Protease Inhibitor Cocktail (P8340). Protein concentration was measured using the Pierce BCA Protein Assay Kit (Thermo Fisher Scientific, Waltham, MA) and 30 mcg were resolved in an SDS-PAGE gel and subjected to immunoblotting using antibodies for Thr389 phospho-S6K1, total S6K1, GAPDH (Cell Signaling Technology, Danvers, MA; 9234, 9202, and 2118, respectively), and anti-Flag (Sigma-Aldrich, F1804).

For cell-cycle experiments, cells were transfected with the different *MTOR* constructs and serum-starved. After trypsinization, cells were fixed with 70% ethanol and intracellularly stained with an anti-FLAG antibody (Sigma-Aldrich), followed by a secondary antimouse Alexa Fluor 647 (Thermo Fisher Scientific), so to identify the positive transfected cells. After the intracellular staining, cells were resuspended in 50 mcg/mL of propidium iodide (Sigma-Aldrich) solution containing 20 mg/mL of ribonuclease A. Cells with the secondary AF647 only were used as staining controls. The cells were analyzed using a FACSCanto II (BD Biosciences, San Jose, CA), pulse processing was used to exclude cell aggregates, and at least 10,000 single cell events were collected. All data were analyzed using FlowJo v10.1 (Tree Star, Ashland, OR).

Histologic Studies

Hematoxylin-eosin–stained and immunohistochemically stained tumor sections were evaluated via

visual examination under a microscope. Immunohistochemistry was performed on tumor tissue sections using antibodies against Ser235/236 phospho-ribosomal protein S6 (p-S6) and Thr202/Tyr204

phospho-ERK (p-ERK) (Cell Signaling Technology; 2211 and 9101, respectively) following standard protocols. The intensity of the staining was evaluated by an experienced pathologist (L.B.).

Reference

1. Apellániz-Ruiz M, Lee MY, Sánchez-Barroso L, et al. Whole-exome sequencing reveals defective CYP3A4 variants predictive of paclitaxel dose-limiting neuropathy. *Clin Cancer Res* 2015;21:322–328.